Microstructure of Hydrogen-Implanted Polycrystalline α-SiC after Annealing *

Hui-Ping Liu(刘会平), Jin-Yu Li(李锦钰)**, Bing-Sheng Li(李炳生)**
Institute of Modern Physics, Chinese Academy of Sciences, Lanzhou 730000

(Received 21 June 2018)

Microstructural evolution in H-implanted polycrystalline α-SiC upon thermal annealing at temperature 1100° C is studied. After annealing, the samples are examined via cross-sectional transmission electron microscopy (XTEM) analysis. H_2 gas bubbles are formed during H implantation and some H_2 molecules are released from the bubble to form cavities during thermal annealing. The distribution and size of the observed cavities are related to the implantation fluence. The results are compared to H implanted single crystal SiC and He implanted polycrystalline α-SiC. The possible reasons are discussed.

PACS: 61.80.Jh, 61.82.Fk, 68.37.Lp, 81.40.Wx DOI: 10.1088/0256-307X/35/9/096103

Silicon carbide (SiC) is regarded as an important material in advanced nuclear energy systems due to the low cross section for neutron capture and its advanced mechanical and chemical stability.[1–4] For example, SiC is a primary candidate material that is composed of tristructural-isotropic (TRISO) coated fuel particles, which can be used in gas-cooled fast reactors and high temperature gas-cooled reactors. Additionally, SiC can be composed of flow channel inserts (FCIs) and structural components for the first wall used in fusion systems. Based on the (n,p) nuclear reaction, large amounts of hydrogen can be produced in fission and fusion systems. Due to the low solubility of hydrogen in SiC, hydrogen is easily trapped at vacancy sites produced by displacement damage to form bubbles. In addition, hydrogen is easily released from bubbles to form cavities under high temperatures.[5] What is more, bubbles and cavities can deteriorate the physical and mechanical properties of SiC materials. Therefore, it is important to investigate the implantation-induced damage in H-implanted SiC.

H-implanted SiC single crystals such as 4H-SiC, 6H-SiC have been extensively investigated.[6–8] The fluence dependence of surface morphology and the threshold fluence for smart-cut in H-implanted 6H-SiC have been investigated by Li *et al.*[6,7] The exfoliation efficiency is related to the implantation-induced defects. The increase of implantation-induced defects can suppress the exfoliation efficiency. The implantation-induced damage and evolution of lattice strain as functions of implantation fluence, temperature, and annealing temperature have also been investigated.[9] Hot-pressed SiC is the most important candidate material in the development of nuclear energy. Therefore, it is important to study the implantation-induced damage in H-implanted hot-pressed SiC. The majority of hot-pressed materials have polycrystalline structures. So far, H-implanted polycrystalline SiC has been less investigated.[9] In this Letter, we report the fluence dependence of the damage formation in the H-implanted polycrystalline α-SiC sample. The microstructural evolution with fluence is observed by cross-sectional transmission electron microscopy (XTEM).

In the present work, samples were hot-pressed polycrystalline α-SiC supplied by the Saint-Gobain company, with a density of 3.1 g/cm^3 and grain sizes of 4–10 μm. Polycrystalline α-SiC contained approximately 90% 6H-SiC and 10% 4H-SiC. Polycrystalline α-SiC samples were implanted with 120 keV H^+ ions with fluences of 1×10^{16}, 3×10^{16}, 5×10^{16}, and 1×10^{17} H^+/cm^2 at room temperature (RT). The implantation experiment was performed at the 320 kV multidisciplinary research platform for highly charged ions of the Institute of Modern Physics, Chinese Academy of Sciences. To study the cavity formation and distribution in the damaged layer, we chose isothermal annealing at temperature 1100°C for 15 min in a vacuum (about 1×10^{-3} Pa). The majority of implanted hydrogen is released in the grain after annealing at 1100°C.

The microstructural evolution of the H-induced damage was studied by means of XTEM using a JEOL 2100 operated at 200 kV. The XTEM samples were prepared by a Hitachi (2000) FIB (focused ion beam) system. Before the FIB process, the implanted surface was protected by depositing a tungsten layer in thickness 1 μm. Fresnel contrast reveals the H-induced cavities. For example, under the under-focus condition, cavities show bright Fresnel fringes, while for over-focus they exhibit dark Fresnel fringes. This phase contrast is related to a change in the electronic potential at the cavities.

Figure 1 presents the distribution of lattice damage in units of displacement per atom (dpa) and the deposited concentration of H into polycrystalline α-SiC sample with 120 keV H^+ ions with a fluence of 5×10^{16} H^+/cm^2, overlaid on the corresponding XTEM bright-field micrograph of the H implanted α-SiC sample. The figure exhibits three distinct regions: (i) a defect-free zone within a depth of ∼71 nm from the sample surface, (ii) a damaged zone with a width of 22+6 nm below the regime (i), and (iii) the virgin substrate below the regime (ii). Note that the depth

*Supported by the National Natural Science Foundation of China under Grant No 11475229.
**Corresponding author. Email: lijinyu@impcas.ac.cn; b.s.li@impcas.ac.cn

region of the damaged layer is located in the depth region of the maximum H deposition as simulated using the Monte-Carlo code SRIM2008 (the density of 3.1 g/cm^3 and the displacement energies of 35 eV for Si and 20 eV for C).[10] It is indicated that implanted hydrogen atoms play an important role in cavity nucleation.

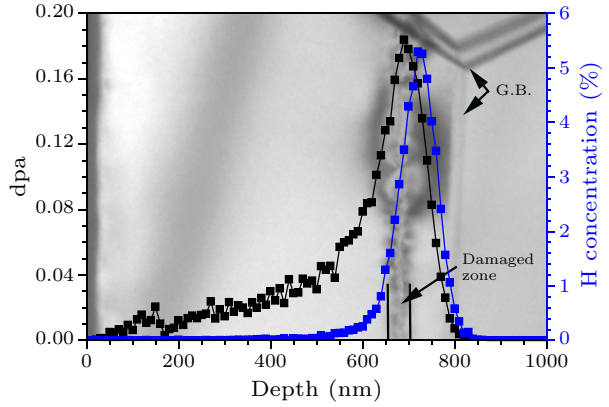

Fig. 1. The distribution of lattice damage in units of displacement per atom (dpa) and the deposited concentration of H in polycrystalline α-SiC implanted with 120 keV H^+ ions with a fluence of 5×10^{16} H^+/cm^2, which overlaid the corresponding XTEM bright-field micrograph of the implanted polycrystalline α-SiC sample.

Figure 2 shows the under-focused XTEM bright field micrographs of the polycrystalline α-SiC samples implanted with H^+ ions with fluences of 1×10^{16}, 3×10^{16}, 5×10^{16}, and 1×10^{17} H^+/cm^2 followed by annealing at 1100°C for 15 min. Note that no cavities and damage contrast can be found in the polycrystalline α-SiC sample implanted with H^+ ions with a fluence of 1×10^{16}/cm^2, as shown in Fig. 2(a). In contrast to He implanted polycrystalline α-SiC sample,[11] our recent report showed that 230 keV He^+ ions implanted polycrystalline α-SiC with a fluence of 1×10^{16}/cm^2, corresponding to the maximum He concentration of 0.65 at.%. After annealing at 1000°C, many He bubbles can be formed in the damaged layer.[11] This different phenomenon is related to the different migration rates between H and He implantation into SiC. Compared with He atoms, the lower desorption temperature and faster migration rate of H atoms in SiC, most of the implanted H atoms are released after annealing at 1100°C for 15 min.[5] For the sample implanted with a fluence of 1×10^{16} H^+/cm^2, the peak damage is only 0.036 dpa and the maximum H concentration is 1.04 at.%. Implanted H atoms can be released and simultaneously H implantation-induced defects can be eliminated during the annealing, and therefore, no lattice damage is found. With increasing fluence with 3×10^{16} H^+/cm^2, cavity distribution is not continuous that only local cavities are found in the damaged layer, as shown in Fig. 2(b). Many cavities migrate and coalesce into cavity clusters that exhibit platelets with a habit plane of (0001). With continuous increasing fluence up to 5×10^{16} H^+/cm^2, cavity distribution is continuous and faceted cavities are found, as shown in Fig. 2(c). Some cavities are considerably large. The width of cavity layer is ~44 nm. The mean size (long axis) and density of observed cavities are 15.3 nm and ~1.4×10^{22}/m^3, respectively. With further increasing implantation to a fluence of 1×10^{17} H^+/cm^2, the morphology and distribution of observed cavities are totally different from those of lower fluences. Dense spherical cavities with a mean diameter of 1.7 nm and a density of ~3.1×10^{23}/m^3 are formed, as shown in Fig. 2(d). Moreover, the width of cavity layer is ~120 nm.

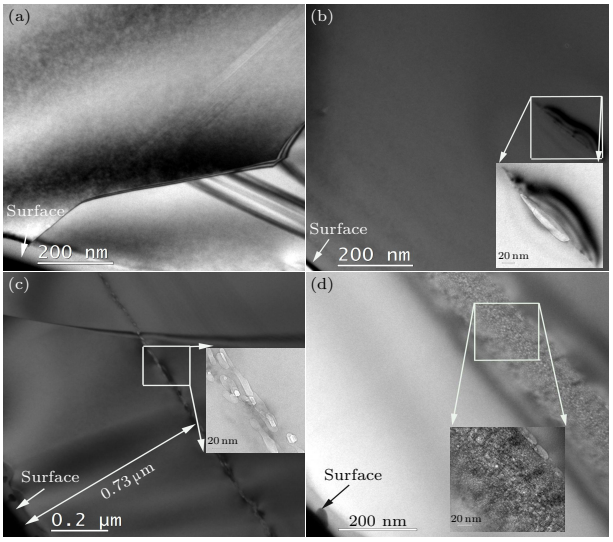

Fig. 2. XTEM bright-field micrographs of the polycrystalline α-SiC samples implanted with 120 keV H ions with fluences of (a) 1×10^{16}, (b) 3×10^{16}, (c) 5×10^{16}, and (d) 1×10^{17}/cm^2 at room temperature and then annealed at 1100°C for 15 min. An under-focused view of the cavity layer distribution in the damage region is performed and the sample surface is shown. The local areas of images (b), (c), and (d) are magnified as shown in the insets.

The formation of faceted cavities is due to the fast migration and coalescence of vacancy-type defects under thermal annealing. Due to the different surface energies, the cavity growth is preferential to growth along the surface with the lower surface energy. Therefore, large and faceted cavities were observed in the sample implanted with H^+ ions with fluences of 3×10^{16} H^+/cm^2 and 5×10^{16} H^+/cm^2. However, for the sample implanted with a fluence of 1×10^{17} H^+/cm^2, H implantation-induced vacancy concentration is two times higher than that of the sample implanted with a fluence of 5×10^{16} H^+/cm^2, numerous implanted H atoms are trapped by vacancy-type defects to form pressurized H_2-gas bubbles. The high inner pressure due to the H_2-gas bubbles implements compressive stress on the nearby silicon carbide lattice, and therefore, bubbles' migration and coalescence are inhibited. It is similar to the case of H implanted single crystal Si.[12] The influence of compressive stress on the migration of pressurized bubbles should be further investigated by theoretical simulation. It can account for the present experimental result that small and spherical cavities with a high density are formed in the sample implanted with a fluence of 1×10^{17} H^+/cm^2. The present experimental results

demonstrate that the threshold fluence of the transition regime of faceted cavities and spherical cavities is located between 5×10^{16} H^+/cm^2 and 1×10^{17} H^+/cm^2. More work is needed to ensure the detailed threshold fluence.

We have studied the 6H-SiC wafers implanted with 134 keV H_2^+ ions with fluences ranging from 1.5×10^{16} H_2^+/cm^2 to 5×10^{16} H_2^+/cm^2 at room temperature.[7] After the implantation, the samples were annealed at a temperature of 1100°C for 15 min. Microcracks can be observed in the samples implanted with fluence of 1.5 and 2.5×10^{16} H_2^+/cm^2 and the damaged layer is amorphous in the sample implanted to a fluence of 5×10^{16} H_2^+/cm^2. In the present experimental results, the microstructure is significantly different from the H_2^+-implanted 6H-SiC. The main reason is due to the polycrystallinity of the SiC used in the present study. The effect of grain boundaries on cavity nucleation should be considered.

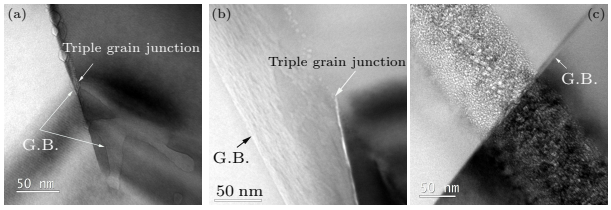

Fig. 3. The under-focused XTEM bright field micrographs of the cavity formation along grain boundaries of the samples implanted with fluences of (a) 3×10^{16}, (b) 5×10^{16}, and (c) $1\times10^{17}/cm^2$ at RT and then annealed at 1100°C for 15 min. Grain boundary (G.B.) was indicated.

Figure 3 shows the under-focused XTEM bright field micrographs taken from grain boundaries of the samples implanted with fluences of 3×10^{16}, 5×10^{16}, and 1×10^{17} H^+/cm^2 followed by annealing at 1100°C for 15 min. To study the effect of grain boundaries on cavity formation, the grain boundary that passes through the maximum damage region is investigated. It can be seen that dense faceted cavities are formed along the grain boundary of the samples implanted with fluences of 3×10^{16} and 5×10^{16} H^+/cm^2. The formation of cavities along the grain boundary is due to the high efficiency of grain boundaries for trapping mobile interstitial H atoms.[13] As a result, numerous H-implantation-induced vacancies migrate, and then recombine with interstitial-type defects, and therefore, only partial vacancies that have the ability to trap implanted H atoms migrate and coalescence to form faceted cavities in the grain interior upon thermal annealing. It is interesting that very large cavities with anomalistic shape were formed in the grain boundary plane. It is indicated that the migration rate of cavities in the grain boundary plane is faster than in the grain interior. The cavity can easily migrate along the grain boundary to escape from the sample when the grain boundary is almost vertical to the sample surface. For the sample implanted with a fluence of 1×10^{17} H^+/cm^2, numerous H-implantation-induced vacancies can trap implanted H atoms to inhibit the trapping of H atoms at the grain boundary. Figure 3(c) shows that there is no preferential cavity nucleation along the grain boundary. Therefore, the influence of grain boundaries on cavity nucleation is related to the H implantation concentration. This is consistent with the He implanted polycrystalline α-SiC.[11]

In conclusion, we have studied the formation of cavities in the H-implanted polycrystalline α-SiC at RT with fluences of 1×10^{16}, 3×10^{16}, 5×10^{16}, and 1×10^{17} H^+/cm^2 followed by annealing at 1100°C for 15 min. The cavity nucleation in grain interiors and along grain boundaries are investigated by XTEM. The implantation-induced damage is completely annealed out for the sample implanted with a fluence of 1×10^{16} H^+/cm^2. Faceted cavities with large sizes are formed in the samples implanted with fluences of 3×10^{16} and 5×10^{16} H^+/cm^2, while spherical cavities with small size are formed in the sample implanted with a fluence of 1×10^{17} H^+/cm^2. The shape and size of cavities are related to the migration rate of vacancy-type defects during thermal annealing. Vacancy-type defects trap implanted H atoms to form pressurized bubbles, which are hard to migrate. The threshold fluence for the transition regime of faceted cavities and spherical cavities is located between 5×10^{16} H^+/cm^2 and 1×10^{17} H^+/cm^2. The detailed threshold fluence will be further investigated in the future. Grain boundaries have a high ability for trapping mobile interstitial H atoms and the ability of trapping H atoms is inversely proportional to the H implantation concentration. As a result, the density of cavities and implantation-induced damage are lower as compared to H implantation into SiC single crystals. There is preferential formation of cavities along grain boundaries for the sample implanted with fluences of 3×10^{16} and 5×10^{16} H^+/cm^2, but not for 1×10^{17} H^+/cm^2.

References

[1] Katoh Y, Snead L L, Henager C H, Hasegawa A, Kohyama A, Riccardi B and Hegeman A 2007 *J. Nucl. Mater.* **367-370** 659
[2] Katoh Y, Snead L L, Szlufarska I and Weber W J 2012 *Curr. Opin. Solid State Mater. Sci.* **16** 143
[3] Snead L L, Nozawa T, Katoh Y, Byun T S, Kondo S and Petti D A 2007 *J. Nucl. Mater.* **371** 329
[4] Snead L L, Nozawa T, Ferraris M, Katoh Y, Shinavski R and Sawan M 2011 *J. Nucl. Mater.* **417** 330
[5] Hasegawa A, Miwa S, Nogami S, Taniguchi A, Taguchi T and Abe K 2004 *J. Nucl. Mater.* **329** 582
[6] Li B S, Wang Z G and Jin J F 2013 *Nucl. Instrum. Methods Phys. Res. Sect.* B **316** 239
[7] Zhang L and Li B S 2017 *Physica* B **508** 104
[8] Hosono T, Hanamto K, Ueno T, Kitabatake I, Sasaki M, Nakayama Y and Nishino S 1999 *Nucl. Instrum. Methods Phys. Res. Sect.* B **149** 67
[9] Hojou K, Furuno S, Kushita K N, Sasajima N and Izui K 1998 *Nucl. Instrum. Methods Phys. Res. Sect.* B **141** 148
[10] http://www.srim.org
[11] Li B S, Du Y Y, Wang Z G, Wei K F, Zhang H P, Yao C F, Chang H L, Sun J R, Cui M H, Sheng Y B, Pang L L, Zhu Y B, Gao X, Luo P, Zhu H P, Wang J and Wang D 2015 *Vacuum* **113** 75
[12] Hochauer T, Misra A, Nastasi M and Mayer J W 2002 *J. Appl. Phys.* **92** 2335
[13] Sun J J, You Y W, Hou J, Li X Y, Li B S, Liu C S and Wang Z G 2017 *Nucl. Fusion* **57** 066031